Enhanced unconventional photon-blockade effect in one- and two-qubit cavities interacting with nonclassical light

H. Jabri [1] and H. Eleuch [2,3]

[1] *Higher Institute of Biotechnology of Beja, University of Jendouba, Beja 9000, Tunisia*
[2] *Department of Applied Physics and Astronomy, University of Sharjah, University City, Sharjah 27272, United Arab Emirates*
[3] *Institute for Quantum Science and Engineering, Texas A&M University, College Station, Texas 77843, USA*

(Received 7 April 2022; revised 15 June 2022; accepted 20 July 2022; published 3 August 2022)

The antibunching effect generated in a cavity containing first a single two-level atomic system and then two identical atoms is explored for off-resonant interactions, in strong- and weak-coupling regimes. The cavity is driven by coherent and squeezed sources. Using the second-order correlation function analytically derived in the weak-excitation regime, we show that squeezed light achieves and improves strong antibunching, leading to a photon blockade. This enhancement is due to a destructive quantum interference mechanism induced by the nonclassical light, creating a supplementary transition pathway. The best effect is obtained for equal frequency detunings in the strong-coupling regime. More interestingly, our investigation reveals that the two-atom-cavity system can further improve the antibunching effect compared to the single-atom cavity. It turns out that the additional couplings appearing in the cavity due to the implementation of the two atoms, combined with the squeezed light, could substantially enhance the photon-blockade effect.

DOI: 10.1103/PhysRevA.106.023704

I. INTRODUCTION

Photon-blockade effects play a crucial role in exchanging and handling photonic quantum information [1–5]. First proposed by Imamoglu *et al.* [6], these intriguing effects have been studied in various systems [7–19]. Generally, a blockade means that the emission of photons can be blocked by a single photon in a cavity. This results in a one by one sequential photon transmission in the output side of the cavity, with sub-Poissonian statistics. In order to obtain photon blockade, a strong quantum nonlinear source is needed. For example, this aspect was studied using a system with an intrinsic nonlinear susceptibility [20–24]. Unfortunately, the requirement of strong nonlinearity is hard to realize experimentally. First discovered by Liew and Savona [25], systems possessing weak nonlinearities can exhibit another type of the photon-blockade phenomenon, known as unconventional photon blockade. The first physical explanations of the unconventional photon blockade were given by Bamba *et al.* [26]. They are underlined by the fact that there are two or more different paths for the transition from the one-photon state to the two-photon state, leading to destructive quantum interference and strong antibunching [27–29]. A unifying interpretation of the conventional and unconventional photon-blockade mechanisms was proposed by Casalengua *et al.* [30].

On the other hand, squeezed states of light constitute a strong resource for several quantum technologies [31,32]. This kind of radiation is characterized by quantum noise in one quadrature lower than a coherent state. The applications include essentially the precision improvement of the optical measurements [33,34], quantum communication [35], gravitational wave detection [36,37], and quantum computing [38–41]. The most notable application of squeezed light was to increase the astrophysical limits of gravitational-wave detectors including the laser interferometer gravitational-wave observatory (LIGO) [42] and the gravitational-wave observatory (GEO 600) detectors [43]. In general, squeezing comes from nonlinear interactions in a quantum system. Widely investigated platforms in quantum optics are the quantum well cavity [44–49] and the two-level atomic system [50–55]. They still offer fascinating behaviors due to their exceptional quantum properties.

In light of this, we investigate in this paper the antibunching effect in a cavity containing first a two-level atomic system and then two atoms. The cavity is doubly pumped by coherent and squeezing sources of light. We show that the antibunching achieved by the single-atom cavity can be strongly enhanced by applying the squeezing source and choosing the appropriate frequency detunings and amplitude of the squeezed light. This improvement is also observed for the two-atom cavity. However, more interestingly, this last system is able to produce higher antibunching than the single-atom case. This is attributed to the additional coupling.

The paper is organized as follows. In the next section we consider the single-atom-cavity system. We derive the Hamiltonian and the dynamics. Then we determine the equal-time second-order correlation function in the weak-excitation regime. After that, we focus on the antibunching effect for weak and strong couplings. Section III is dedicated to the two-atom-cavity system. We study the antibunching and take the opportunity to compare the nonclassical effect generated by the two systems. In the Appendix we extend the study of the single-atom cavity to off-resonant interactions.

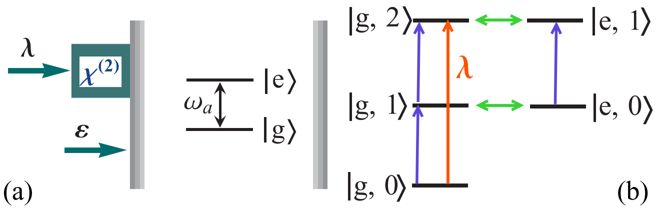

FIG. 1. (a) Scheme of a two-level system trapped in a single-mode cavity. The cavity is coherently pumped by a laser of amplitude ε. A second-order nonlinear crystal is attached to the cavity in such a way that the generated squeezed photons interact with the two-level system. (b) Transition paths for different photon states induced by coherent and squeezed sources.

II. ONE-QUBIT-CAVITY SYSTEM

A. Theoretical model and dynamics

We consider an optical cavity (with a mode frequency ω_c) containing a two-level system (of frequency ω_a), weakly driven by a coherent field. The cavity interacts with squeezed photons that result from a nonlinear process through a second-order nonlinear crystal attached to the cavity, as shown schematically in Fig. 1(a). We note that our discussion deals with a general model that can be realized in several quantum systems, such as atom-cavity systems, superconducting qubit-cavity systems, and quantum-dot cavities. The whole Hamiltonian describing the system, in a rotating frame, can be written as

$$\begin{aligned} H_1 =& \Delta_c a^\dagger a + \Delta_a \sigma^\dagger \sigma + g(\sigma a^\dagger + \sigma^\dagger a) \\ &+ (\varepsilon a^\dagger + \bar{\varepsilon} a) + \left(\frac{\lambda}{2} a^{\dagger 2} + \frac{\bar{\lambda}}{2} a^2\right), \end{aligned} \quad (1)$$

where a and $a^\dagger$ represent the annihilation and creation operators of the optical mode of the cavity, respectively, σ and $\sigma^\dagger$ denote the lowering and raising operators of the two-level atomic system, respectively, and ε is the strength of the coherent driving field and $\bar{\varepsilon}$ its complex conjugate. The interaction strength between photons and the atom is represented by the constant g. The second-order medium of susceptibility $\chi^{(2)}$ is driven by a field of amplitude λ_p. They are linked by the relation $\lambda = \chi^{(2)}\lambda_p$. Here $\Delta_a = \omega_a - \omega_p$ and $\Delta_c = \omega_c - \omega_p$ are the two-level system and cavity detunings with respect to the driving pump frequency, respectively.

The system dynamics can be analyzed with the master equation for the density matrix ρ, given by $\dot{\rho}(t) = i[\rho, H_1] + \kappa \mathcal{L}_a[\rho] + \gamma \mathcal{L}_\sigma[\rho]$, where $\mathcal{L}_a[\rho] = 2a\rho a^\dagger - a^\dagger a \rho - \rho a^\dagger a$ and $\mathcal{L}_\sigma[\rho] = 2\sigma\rho\sigma^\dagger - \sigma^\dagger\sigma\rho - \rho\sigma^\dagger\sigma$ are the Lindblad superoperators describing the dissipations of the cavity and the two-level system with the decay rates κ and γ, respectively. By adopting the weak-driving limit, the system wave function can be expanded in terms of the bare states up to a two-photon excitation process as [56,57]

$$\begin{aligned} |\psi\rangle \approx& A_{g,0}|g, 0\rangle + A_{g,1}|g, 1\rangle + A_{g,2}|g, 2\rangle \\ &+ A_{e,0}|e, 0\rangle + A_{e,1}|e, 1\rangle. \end{aligned} \quad (2)$$

In this representation, the quantities $|A_{g,n}|^2$ and $|A_{e,n}|^2$ constitute the probabilities of the system in the states $|g, n\rangle$ and $|e, n\rangle$, respectively. Under these conditions, the system is described by the effective non-Hermitian Hamiltonian

$$H_1' = H_1 - i\frac{\kappa}{2} a^\dagger a - i\frac{\gamma}{2}\sigma^\dagger\sigma. \quad (3)$$

To obtain the evolution equations of the amplitudes $A_{\alpha,n}$ ($\alpha = g, e$), we employ the Schrödinger equation $i\partial_t|\psi\rangle = H_1'|\psi\rangle$. Combining Eqs. (2) and (3) into the Schrödinger equation, we obtain the set of equations relative to the coefficients of the wave function

$$i\dot{A}_{g,1} = \varepsilon + gA_{e,0} + \Delta_c' A_{g,1} + \sqrt{2}\bar{\varepsilon} A_{g,2}, \quad (4)$$

$$i\dot{A}_{g,2} = \sqrt{2} g A_{e,1} + 2\Delta_c' A_{g,2} + \sqrt{2}\varepsilon A_{g,1} + \frac{\sqrt{2}}{2}\lambda, \quad (5)$$

$$i\dot{A}_{e,0} = gA_{g,1} + \Delta_a' A_{e,0} + \sqrt{2}\bar{\varepsilon} A_{e,1}, \quad (6)$$

$$i\dot{A}_{e,1} = \sqrt{2} g A_{g,2} + (\Delta_a' + \Delta_c')A_{e,1} + \varepsilon A_{e,0}, \quad (7)$$

with $\Delta_a' = \Delta_a - i\gamma/2$ and $\Delta_c' = \Delta_c - i\kappa/2$. Under the weak-driving condition $|A_{g,0}| \gg |A_{g,1}|, |A_{e,0}| \gg |A_{g,2}|, |A_{e,1}|$, the steady-state solutions ($\partial_t A_{\alpha,n} = 0$) for the amplitudes of each state are given by

$$\begin{aligned} A_{g,1}\mathcal{B} =& \bar{\varepsilon}[\lambda\Delta_a'(\Delta_a' + \Delta_c') + \sqrt{2}(2\varepsilon^2\Delta_c' + g^2\lambda)] \\ &- \varepsilon\{\sqrt{2}\lambda\bar{\varepsilon}^2 + 2\Delta_a'[\Delta_c'(\Delta_a' + \Delta_c') - g^2]\}, \end{aligned} \quad (8)$$

$$\begin{aligned} A_{g,2}\mathcal{B} =& \frac{g^2}{\sqrt{2}}[\lambda(\Delta_a' + \Delta_c') + 2\varepsilon^2] \\ &- \frac{2\varepsilon^2 - \lambda\Delta_c'}{\sqrt{2}}[\sqrt{2}|\varepsilon|^2 - \Delta_a'(\Delta_a' + \Delta_c')], \end{aligned} \quad (9)$$

$$A_{e,0}\mathcal{B} = 2g\varepsilon[\Delta_c'(\Delta_a' + \Delta_c') - g^2], \quad (10)$$

$$A_{e,1}\mathcal{B} = g[\lambda|\varepsilon|^2 + \Delta_a'(\lambda\Delta_c' - 2\varepsilon^2) - 2\varepsilon^2\Delta_c' - g^2\lambda], \quad (11)$$

where

$$\begin{aligned} \mathcal{B} =& 2g^4 + 2\big(|\varepsilon|^2 - \Delta_c'^2\big)[\sqrt{2}|\varepsilon|^2 - \Delta_a'(\Delta_a' + \Delta_c')] \\ &- 2g^2[(\sqrt{2}+1)|\varepsilon|^2 + \Delta_c'(2\Delta_a' + \Delta_c')]. \end{aligned} \quad (12)$$

B. Second-order correlation function determination

Usually, to study the quantum statistics of the optical cavity field we use the equal-time second-order correlation function $g^{(2)}(0)$, which is proportional to the probability of detecting two photons simultaneously. Its value determines the nature of the produced light: $g^{(2)}(0) = 1$ for coherently emitted radiation and $g^{(2)}(0) > 1$ for super-Poissonian bunched light, whereas when $g^{(2)}(0) < 1$ the field statistics are sub-Poissonian corresponding to antibunched or nonclassical light. In particular, the value $g^{(2)}(0) \ll 1$ is a signature of the photon-blockade phenomenon, when only one-photon excitation is possible. The steady-state second-order correlation function of the cavity optical field can be written as

$$g^{(2)}(0) = \frac{\langle\psi|a^\dagger a^\dagger a a|\psi\rangle_{SS}}{\langle\psi|a^\dagger a|\psi\rangle_{SS}^2}, \quad (13)$$

where $|\psi\rangle_{SS}$ is the system wave function in the steady state. The stationary values are linked to the mean value of number of photons by $\langle\psi|a^\dagger a|\psi\rangle_{SS} = |A_{g,1}|^2 + |A_{e,1}|^2 + 2|A_{g,2}|^2$, from which the autocorrelation function for weak excitation takes the form [after considering real ε in Eqs. (8) and (9) in order to simplify the study of $g^{(2)}(0)$]

$$g^{(2)}(0) = \frac{|\sqrt{2}A_{g,2}|^2}{[|A_{g,1}|^2 + |A_{e,1}|^2 + 2|A_{g,2}|^2]^2} \simeq \frac{2|A_{g,2}|^2}{|A_{g,1}|^4} = \frac{N_1 + N_2}{N_3|\mathcal{D}|^2}, \tag{14}$$

with

$$N_1 = \Big(\tfrac{1}{4}\big\{\Delta_a^2(8\varepsilon^2 - 4\lambda\Delta_c) + \Delta_a\big[-4\lambda\Delta_c^2 + 8\varepsilon^2\Delta_c + \kappa\lambda(2\gamma+\kappa) + 4g^2\lambda\big] + \lambda\Delta_c[\gamma(\gamma+2\kappa) + 4g^2] + 2\varepsilon^2[4g^2 - \gamma(\gamma+\kappa)]\big\}\Big)^2, \tag{15}$$

$$N_2 = \Big(\tfrac{1}{8}\big\{8\Delta_a[\lambda\Delta_c(\gamma+\kappa) - \varepsilon^2(2\gamma+\kappa)] + 4\kappa\lambda\Delta_a^2 + 4\gamma\Delta_c(\lambda\Delta_c - 2\varepsilon^2) - \lambda(\gamma+\kappa)(\gamma\kappa+4g^2)\big\}\Big)^2, \tag{16}$$

$$N_3 = \left[\frac{4\varepsilon^2\big(4\Delta_a^2+\gamma^2\big)}{4(\kappa\Delta_a+\gamma\Delta_c)^2 + (-4\Delta_a\Delta_c + \gamma\kappa + 4g^2)^2}\right]^2, \tag{17}$$

and

$$\mathcal{D} = \tfrac{1}{8}[2i\Delta_a(\kappa + 2i\Delta_c) + 2i\gamma\Delta_c + \gamma\kappa + 4g^2] \times [2i\Delta_a(\kappa+2i\Delta_c) + 2i\Delta_c(2i\Delta_c + \gamma + 2\kappa) + \kappa(\gamma+\kappa) + 4g^2]. \tag{18}$$

The above general relation of the autocorrelation function characterizes the quantum statistics and the degree of antibunching in the emergent light. According to Eq. (14), if $A_{g,2} = 0$, we have $g^{(2)}(0) = 0$. Thus, in this particular case, light will exhibit strong antibunching, leading to an optimum photon blockade.

C. Quantum-interference-based photon blockade induced by squeezed light for the one-qubit cavity

As mentioned earlier, the two-level atomic system is a good prototype to produce the photon-blockade effect, either by strong nonlinearity between polaritons, qualified as conventional photon blockade (CPB), or via a quantum interference mechanism, known as unconventional photon blockade (UCPB). Despite their mechanisms being different, CPB and UCPB share the same photon quantum statistics. Here we explore the effect of the squeezed light on the antibunching effect produced by the two-level cavity system. For this, we begin with the total resonance case ($\Delta_a = \Delta_c = 0$). The correlation function is reduced to

$$g^{(2)}(0) = \frac{\lambda^2\alpha + 16\varepsilon^4(\gamma\kappa+4g^2)^2[\gamma(\gamma+\kappa) - 4g^2]^2}{16\gamma^4\varepsilon^4[\kappa(\gamma+\kappa)+4g^2]^2}, \tag{19}$$

with $\alpha = (\gamma+\kappa)^2(\gamma\kappa+4g^2)^4$. We note that the previous correlation function depends on the amplitude of the coherent pumping ε, contrarily to the correlation function in the absence of the squeezing source. To illustrate the above expression, we represent in Fig. 2 $g^{(2)}(0)$ against the normalized coupling strength g/κ for three values of the squeezed light amplitude λ/κ. For the system parameters, we choose

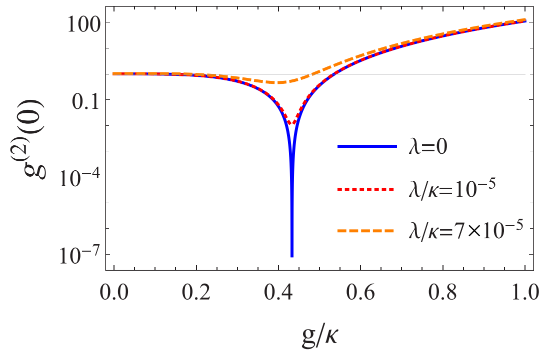

FIG. 2. Second-order correlation function $g^{(2)}(0)$ plotted at total resonance ($\Delta_a = \Delta_c = 0$) as a function of the normalized coupling strength g/κ for $\varepsilon/\kappa = 0.01$, $\gamma = \kappa/2$, and three values of the squeezed light amplitude λ.

$\varepsilon = 0.01\kappa$ and $\gamma = \kappa/2$. The plot shows that for $\lambda = 0$, a strong antibunching effect of the order of 10^{-4} can be attained. As λ increases, the antibunching decreases and vanishes progressively for stronger squeezed pumping. Indeed, at total resonance, the squeezed light is unfavorable to the photon blockade (PB). This is well justified by the optimal condition for the photon blockade derived from Eq. (19), satisfying $\lambda = 0$ and $g = \frac{1}{2}\sqrt{\gamma(\gamma+\kappa)}$.

Now we consider resonance between the cavity and the driving field, $\Delta_c = 0$. In Fig. 3(a) we depict the autocorrelation function versus Δ_a/κ in the weak-coupling regime ($g \ll \kappa, \gamma$). We choose the atom-cavity coupling strength

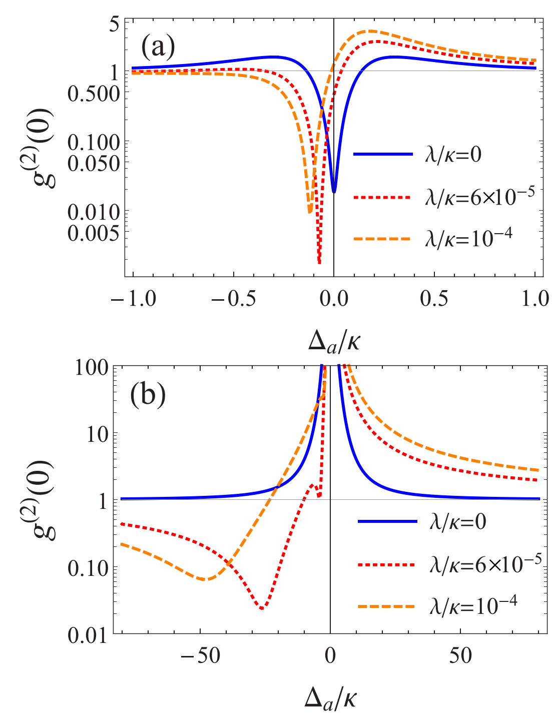

FIG. 3. Second-order correlation function $g^{(2)}(0)$ plotted versus normalized detuning Δ_a/κ ($\Delta_c = 0$) for $\gamma = \kappa/2$, $\varepsilon/\kappa = 0.01$, and three values of the squeezed light strength λ are considered in (a) the weak-coupling regime $g/\kappa = 0.45$ and (b) the strong-coupling regime $g/\kappa = 10$.

$g = 0.45\kappa$. It is shown that for an appropriate value of the squeezed photons amplitude, the PB can be strongly enhanced. However, by further increasing λ, the nonclassical effect decreases. Additionally, we observe that $g^{(2)}(0)$ is redshifted and the maxima no longer correspond to the resonance. The strong-coupling regime ($g \gg \kappa, \gamma$) is illustrated by Fig. 3(b). The coupling strength is chosen to be $g = 10\kappa$. Starting from $\lambda = 0$, light shows highly bunched states near resonance [$g^{(2)}(0) \gg 1$] or coherent states for large detunings [$g^{(2)}(0) \to 1$]. Interestingly, when squeezed photons come into play and even for small nonlinearities, a strong antibunching can be achieved in the region where the coherent pumping frequency is higher than the atomic one ($\omega_a < \omega_p$).

The optimal conditions for PB are derived from the limit $g^{(2)}(0) \to 0$. This means that the real and imaginary parts of Eq. (9) should be equal to zero. Thus, we obtain a set of two equations with variables λ and Δ_a. Solving this system, under the weak-excitation condition $|\varepsilon| \ll \kappa$, yields four solutions for the couples (λ, Δ_a) as

$$\begin{aligned}\lambda_{1,2} &= \pm i\frac{\sqrt{2(\beta + 2\gamma^2\kappa + 2\gamma\kappa^2 + \kappa^3) + 8g^2(\gamma+\kappa)}}{\sqrt{\kappa}(\gamma+\kappa)(\gamma\kappa+4g^2)[\kappa(2\gamma+\kappa)+4g^2]} \\ &\quad \times [-\beta + \kappa(2\gamma+\kappa)^2 + 12g^2(\gamma+\kappa)]\varepsilon^2, \\ \Delta_{a,1,2} &= \mp\frac{\sqrt{-\beta - \kappa(2\gamma^2 + 2\gamma\kappa + \kappa^2) - 4g^2(\gamma+\kappa)}}{2\sqrt{2}};\end{aligned} \tag{20}$$

$$\begin{aligned}\lambda_{3,4} &= \pm i\frac{\sqrt{2(-\beta + 2\gamma^2\kappa + 2\gamma\kappa^2 + \kappa^3) + 8g^2(\gamma+\kappa)}}{\sqrt{\kappa}(\gamma+\kappa)(\gamma\kappa+4g^2)[\kappa(2\gamma+\kappa)+4g^2]} \\ &\quad \times [-\beta + \kappa(2\gamma+\kappa)^2 + 12g^2(\gamma+\kappa)]\varepsilon^2, \\ \Delta_{a,3,4} &= \mp\frac{\sqrt{\beta - \kappa(2\gamma^2 + 2\gamma\kappa + \kappa^2) - 4g^2(\gamma+\kappa)}}{2\sqrt{2}},\end{aligned} \tag{21}$$

where $\beta = [\kappa^4(2\gamma+\kappa)^2 + 16g^4(\gamma+\kappa)(\gamma+5\kappa) + 8g^2\kappa^2(\gamma+\kappa)(2\gamma+\kappa)]^{1/2}$.

From Eq. (9), optimal λ could be real or complex depending on the phase of the pump laser, $\varepsilon = \varepsilon' e^{i\varphi}$ and $\bar{\varepsilon} = \varepsilon' e^{-i\varphi}$. For an appropriate choice of phase angle, $\lambda_{3,4}$, for example, are real solutions. These solutions are plotted as a function of the coupling strength in Fig. 4 with the frequency detunings $\Delta_{a,3,4}$. Obviously, the total resonance conditions are included and observed in these figures. The most important ascertainment is that for weak or intermediate couplings, a quasiresonant excitation and a relatively strong second-order nonlinearity are needed to achieve optimal PB. However, in the strong-coupling regime, a very weak nonlinearity is sufficient, but for large detunings, to obtain optimal PB. The two parameters vary oppositely and are compensated by each other. This optimal condition behavior explains the differences between the weak and strong couplings observed in Fig. 3, especially for the increasing detuning.

Here we consider resonance between the two-level system and the driving field ($\Delta_a = 0$). For weak coupling [Fig. 5(a)], the squeezed light highly increases the blockade of photons where the peaks of $g^{(2)}(0)$ are also redshifted. A stronger pumping λ reduces the antibunching (dashed line). In addition, the antibunching appears in another range of Δ_c/κ away from resonance (dotted line). Unfortunately, in the strong-coupling regime, the interaction with the nonlinear crystal is always favorable to higher bunched states of light [Fig. 5(b)].

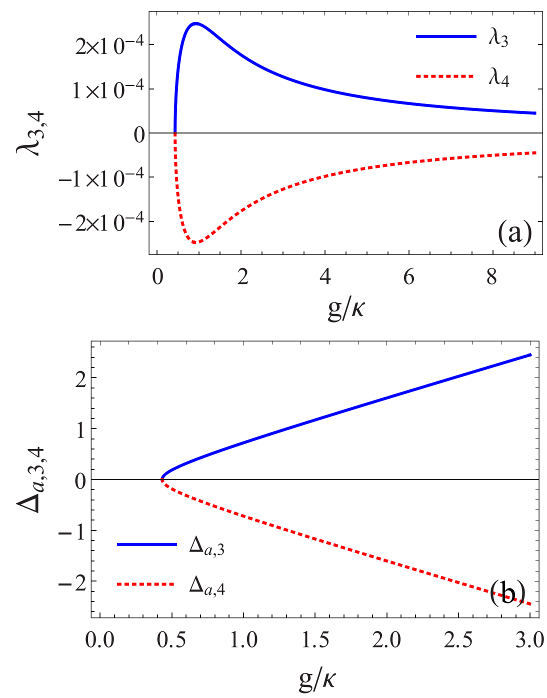

FIG. 4. Optimal PB conditions for (a) squeezed light amplitude $\lambda_{3,4}$ and (b) detunings $\Delta_{a,3,4}$ plotted as a function of the coupling strength g/κ for $\gamma = \kappa/2$ and $\varepsilon/\kappa = 0.01$.

In this case, optimal PB conditions for λ and Δ_c read

$$\begin{aligned}\lambda_{1,2} &= \pm\frac{\varepsilon^2\{4\sqrt{\gamma(\gamma\kappa+8g^2)}[4g^2 - \gamma(\gamma+\kappa)]\}}{[\gamma(\gamma+2\kappa)+4g^2]\sqrt{(\gamma+\kappa)(\gamma\kappa+4g^2)}}, \\ \Delta_{c,1,2} &= \mp\frac{\sqrt{(\gamma+\kappa)(\gamma\kappa+4g^2)[4g^2-\gamma(\gamma+\kappa)]}}{2\sqrt{\gamma(\gamma\kappa+8g^2)}}.\end{aligned}$$

For strong coupling, $\lambda_{1,2}$ can be approximated simply to $\lambda_{1,2} \simeq \pm 2\sqrt{2\gamma}\varepsilon^2/(g\sqrt{\gamma+\kappa})$. For weak coupling, they are given by $\lambda_{1,2} \simeq \pm 4i\varepsilon^2/(\gamma+2\kappa)$. Both solutions also could be complex via adjusting the phase. Plots of these conditions show behavior similar to the previous case when $\Delta_a = 0$ (figures are not shown here).

For a more generalized situation, we examine the case of equal detunings ($\Delta_a = \Delta_c = \Delta$). A very strong antibunching is obtained in the weak-coupling regime at $\Delta = 10\kappa, 20\kappa$ [Fig. 6(a)] and especially in the strong-coupling regime for larger detunings $\Delta = 100\kappa, 200\kappa$ [Fig. 6(b)]. In the latter regime, the antibunching effect increases considerably: The value of $g^{(2)}(0)$ changes from 10^{-1} to a value close to 10^{-5}, which corresponds to an almost perfect photon blockade. An extension to off-resonant interactions $\Delta_a \neq \Delta_c$ is given in the Appendix.

Full analytical solutions for optimal PB conditions of this situation are too long to be presented here. However, it is

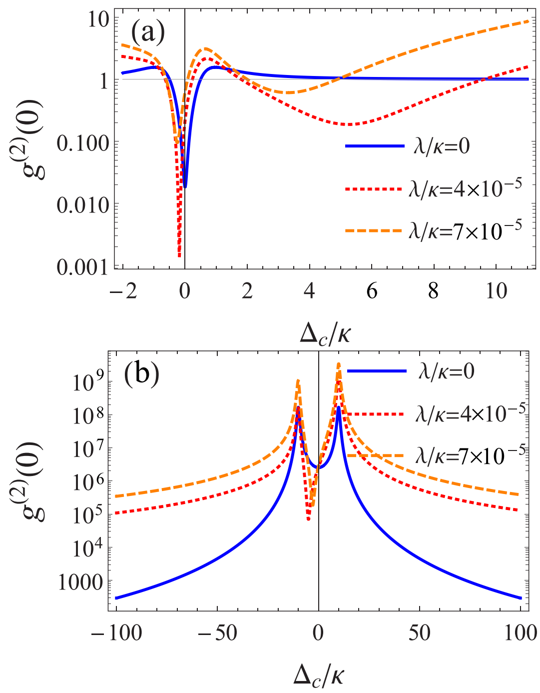

FIG. 5. Second-order correlation function $g^{(2)}(0)$ plotted as a function of the normalized detuning Δ_c/κ ($\Delta_a = 0$) for $\gamma = \kappa/2$, $\varepsilon/\kappa = 0.01$, and three values of λ in (a) the weak-coupling regime $g/\kappa = 0.45$ and (b) the strong-coupling regime $g/\kappa = 10$.

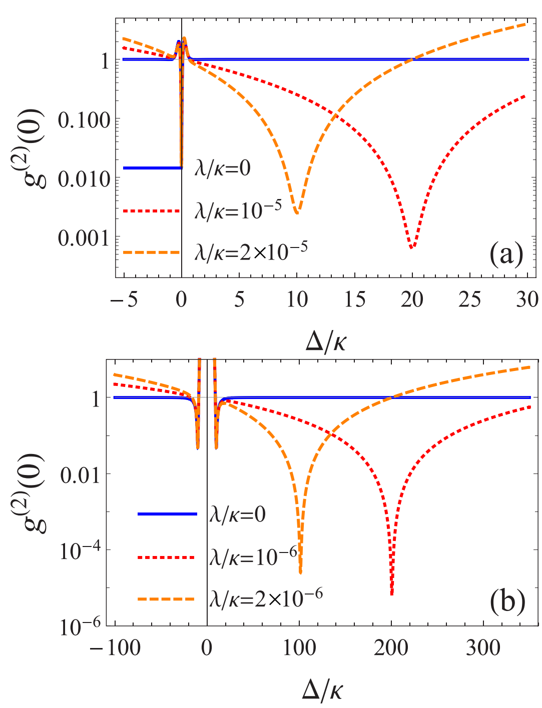

FIG. 6. Second-order correlation function $g^{(2)}(0)$ plotted versus the normalized detuning Δ/κ for $\gamma = \kappa/2$, $\varepsilon/\kappa = 0.01$, and several values of λ in (a) the weak-coupling regime $g/\kappa = 0.45$ and (b) the strong-coupling regime $g/\kappa = 10$.

possible to obtain simple approximated relations for strong coupling as

$$\lambda_{1,2} = \pm\frac{\varepsilon^2[(21\gamma + 17\kappa) - 3\xi]\sqrt{(7\gamma + 3\kappa) + \xi}}{8g\sqrt{2\kappa}(\gamma + \kappa)},$$
$$\Delta_{1,2} = \mp\frac{\sqrt{(7\gamma + 3\kappa) + \xi}}{2\sqrt{2\kappa}}g; \tag{22}$$
$$\lambda_{3,4} = \pm\frac{\varepsilon^2[(21\gamma + 17\kappa) + 3\xi]\sqrt{(7\gamma + 3\kappa) + \xi}}{8g\sqrt{2\kappa}(\gamma + \kappa)},$$
$$\Delta_{3,4} = \mp\frac{\sqrt{(7\gamma + 3\kappa) - \xi}}{2\sqrt{2\kappa}}g, \tag{23}$$

where $\xi = (49\gamma^2 + 58\gamma\kappa + 25\kappa^2)^{1/2}$, and weak coupling as

$$\lambda_{1,2} = \pm i\frac{(5\gamma + 3\kappa) - 3(\gamma - \kappa)}{(\gamma + \kappa)(\gamma + 3\kappa)}\varepsilon^2,$$
$$\Delta_{1,2} = \mp\frac{\sqrt{\kappa(-5\gamma^2 + 2\gamma\kappa + \kappa^2) + \eta}}{4\sqrt{2\kappa}}; \tag{24}$$
$$\lambda_{3,4} = \pm i\frac{(5\gamma + 3\kappa) + 3(\gamma - \kappa)}{(\gamma + \kappa)(\gamma + 3\kappa)}\varepsilon^2,$$
$$\Delta_{3,4} = \mp\frac{\sqrt{\kappa(-5\gamma^2 + 2\gamma\kappa + \kappa^2) - \eta}}{4\sqrt{2\kappa}}, \tag{25}$$

where $\eta = (\gamma - \kappa)(3\gamma + \kappa)$. These conditions behave similarly to those discussed above.

When there is no external squeezed source applied to the system, we have two different transition pathways that correspond to the transition from $|g, 1\rangle$ to $|g, 2\rangle$: the direct excitation $|g, 1\rangle \to |g, 2\rangle$ and the coupling-mediated transition $|g, 1\rangle \to |e, 0\rangle \to |e, 1\rangle \to |g, 2\rangle$. The insertion of the optical parametric oscillator medium results in the creation of a third pathway transition directly from the ground state $|g, 0\rangle$ to $|g, 2\rangle$ ensured by the parameter λ, as shown in Fig. 1(b). Consequently, the improvement of PB outlined above is attributed to this additional transition, making destructive quantum interference stronger. On the other hand, the squeezed interaction may lead also to a constructive quantum interference which explains the high bunching.

III. TWO-QUBIT CAVITY SYSTEM

A. Theoretical model and dynamics

In this section we consider two identical two-level systems trapped in a cavity. We assume that the coupling strengths between atoms and light are the same. The total Hamiltonian is written as

$$H_2 = \Delta_c a^\dagger a + \sum_{j=1}^{2}[\Delta_a\sigma_j^\dagger\sigma_j + g(\sigma_j a^\dagger + \sigma_j^\dagger a)] + (\varepsilon a^\dagger + \bar{\varepsilon} a) + \left(\frac{\lambda}{2}a^{\dagger 2} + \frac{\bar{\lambda}}{2}a^2\right), \tag{26}$$

where j designates the jth two-level system. Then the master equation governing the system dynamics can be expressed as

$$\dot{\rho}(t) = i[\rho, H_2] + \kappa\mathcal{L}_a[\rho] + \sum_{j=1}^{2}\gamma\mathcal{L}_\sigma^{(j)}[\rho], \tag{27}$$

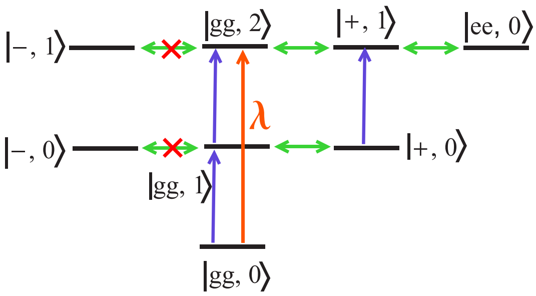

FIG. 7. Transition pathways in the two-atom cavity system in the presence of squeezed light. The antisymmetric Dicke states $|-,0\rangle$ and $|-,1\rangle$ are dark states, decoupled from the other states of the system.

where $\mathcal{L}_\sigma^{(j)}[\rho]$ denotes the dissipation term of the jth two-level system. The whole system can be derived using the collective states $\{|gg\rangle, |\pm\rangle, |ee\rangle\}$ as the basis. In this representation, the states $|\pm\rangle = (|eg\rangle \pm |ge\rangle)/\sqrt{2}$ are the symmetric and antisymmetric Dicke states, respectively. Then the system wave function can written as

$$|\psi\rangle \approx \sum_{n=0}^{2} A_{gg,n}|gg,n\rangle + \sum_{n=0}^{1} A_{\pm,n}|\pm,n\rangle + A_{ee,0}|ee,0\rangle. \quad (28)$$

Transition pathways are shown in Fig. 7. The evolution equations of the wave-function coefficients can then be deduced as

$$i\dot{A}_{gg,1} = \sqrt{2}gA_{+,0} + \Delta'_c A_{gg,1} + \varepsilon + \sqrt{2}\bar{\varepsilon}A_{gg,2}, \quad (29)$$

$$i\dot{A}_{gg,2} = 2gA_{+,1} + 2\Delta'_c A_{gg,2} + \sqrt{2}\varepsilon A_{gg,1} + \frac{\sqrt{2}}{2}\lambda, \quad (30)$$

$$i\dot{A}_{+,0} = \Delta'_a A_{+,0} + \sqrt{2}gA_{gg,1} + \bar{\varepsilon}A_{+,1}, \quad (31)$$

$$i\dot{A}_{+,1} = (\Delta'_a + \Delta'_c)A_{+,1} + 2gA_{gg,2} + \sqrt{2}gA_{ee,0} + \varepsilon A_{+,0}, \quad (32)$$

$$i\dot{A}_{ee,0} = 2\Delta'_a A_{ee,0} + \sqrt{2}gA_{+,1}, \quad (33)$$

with Δ'_a and Δ'_c defined earlier in Sec. II. By solving the previous set under the steady-state approximation, we obtain for the amplitudes

$$\begin{aligned} A_{gg,1}\mathcal{C} = {} & 2\bar{\varepsilon}\Delta'_a[\lambda\Delta'_a(\Delta'_a + \Delta'_c) + 2\varepsilon^2\Delta'_c + g^2\lambda] \\ & - 2\varepsilon\Delta'_a\big[\lambda\bar{\varepsilon}^2 + 2\Delta'^2_a\Delta'_c + 2\Delta'_a(\Delta'^2_c - 2g^2) - 2g^2\Delta'_c\big], \end{aligned} \quad (34)$$

$$\begin{aligned} A_{+,0}\mathcal{C} = {} & 2\sqrt{2}g\bar{\varepsilon}[g^2\lambda - \Delta'_a(\lambda\Delta'_a + 2\lambda\Delta'_c - 2\varepsilon^2)] \\ & + 4\sqrt{2}g\varepsilon\big[\Delta'^2_a\Delta'_c + \Delta'_a\big(\Delta'^2_c - 2g^2\big) - g^2\Delta_c\big], \end{aligned} \quad (35)$$

$$A_{ee,0}\mathcal{C} = 2g^2[-\lambda|\varepsilon|^2 + \Delta'_a(2\varepsilon^2 - \lambda\Delta'_c) + 2\varepsilon^2\Delta'_c + 2g^2\lambda], \quad (36)$$

$$\begin{aligned} A_{+,1}\mathcal{C} = {} & 2\sqrt{2}g\Delta'_a \\ & \times [\lambda|\varepsilon|^2 + \Delta'_a(\lambda\Delta'_c - 2\varepsilon^2) - 2(\varepsilon^2\Delta'_c + g^2\lambda)], \end{aligned} \quad (37)$$

$$\begin{aligned} A_{gg,2}\mathcal{C} = {} & \sqrt{2}g^2\{\Delta'_a[\lambda(2\Delta'_a + 3\Delta'_c) + 2\varepsilon^2] - 2g^2\lambda\} \\ & - \sqrt{2}\Delta'_a(2\varepsilon^2 - \lambda\Delta'_c)[|\varepsilon|^2 - \Delta'_a(\Delta'_a + \Delta'_c)], \end{aligned} \quad (38)$$

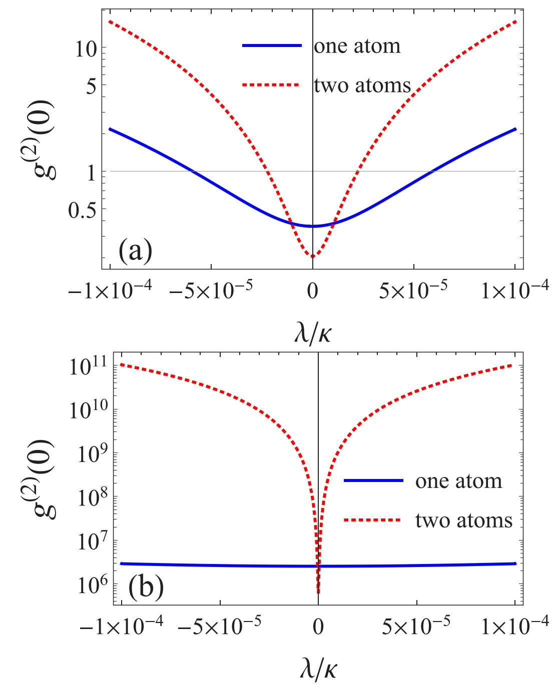

FIG. 8. Plots of the second-order correlation function $g^{(2)}(0)$ at total resonance ($\Delta_a = \Delta_c = 0$) as a function of the normalized squeezed light strength λ/κ for the two systems considered for the parameters $\varepsilon/\kappa = 0.01$ and $\gamma = \kappa/2$ in (a) the weak-coupling regime case ($g = 0.5\kappa$) and (b) the strong-coupling regime ($g = 10\kappa$).

where

$$\begin{aligned} \mathcal{C} = {} & 4\Delta'^2_a\big[(\Delta'_a + \Delta'_c)\big(\Delta'^2_c - |\varepsilon|^2\big) - 4g^2\Delta'_c\big] + 8g^4\Delta'_c \\ & + 4\Delta'_a\big[-\Delta'^2_c(|\varepsilon|^2 + 3g^2) + |\varepsilon|^2(|\varepsilon|^2 - 3g^2) + 4g^4\big]. \end{aligned} \quad (39)$$

B. Quantum-interference-based photon blockade induced by squeezed light for the two-qubit cavity

At total resonance where coherent drive, cavity, and atomic frequencies are equal, the correlation function is written as (for simplicity, here ε is considered real)

$$\begin{aligned} g^{(2)}(0) & \simeq \frac{2|A_{gg,2}|^2}{|A_{gg,1}|^4} \\ & \simeq \frac{(\gamma\kappa + 8g^2)^2\{16\gamma^2\varepsilon^4[\gamma(\gamma+\kappa) - 4g^2]^2 + Z\}}{16\gamma^4\varepsilon^4[\gamma\kappa(\gamma+\kappa) + 4g^2(2\gamma+\kappa)]^2}, \end{aligned} \quad (40)$$

where $Z = \lambda^2(\gamma\kappa + 8g^2)^2[\gamma(\gamma+\kappa) + 4g^2]^2$. From Eq. (40) we can see that the two-atom cavity satisfies the same optimum condition as the single-atom case, particularly the condition $\lambda = 0$. This is clearly observed in Fig. 8(a), which represents $g^{(2)}(0)$ versus λ/κ for weak coupling. It is shown that maximal antibunching appears as a single peak when no squeezed light is injected. Otherwise, squeezed light decreases the antibunching effect. For this resonant interaction, there are three different pathways for two-photon excitation. The first transition is $|gg,1\rangle \rightarrow |gg,2\rangle$, the second one is $|gg,1\rangle \rightarrow |+,0\rangle \rightarrow (|+,1\rangle \leftrightarrow |ee,0\rangle) \rightarrow |gg,2\rangle$, and the

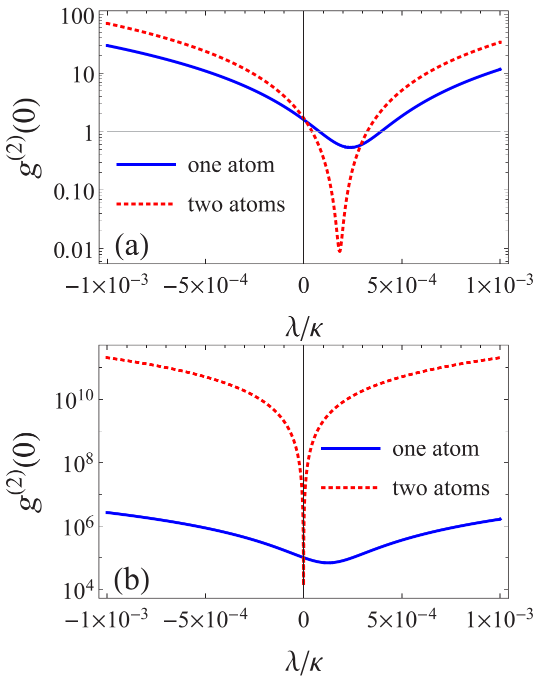

FIG. 9. Second-order correlation function $g^{(2)}(0)$ plotted versus of the normalized strength of squeezed light λ/κ for the two systems ($\Delta_c = 0$ and $\Delta_a = -0.5\kappa$) for the parameters $\varepsilon/\kappa = 0.01$ and $\gamma = \kappa/2$ in (a) the weak-coupling regime ($g = 0.5\kappa$) and (b) the strong-coupling regime ($g = 10\kappa$).

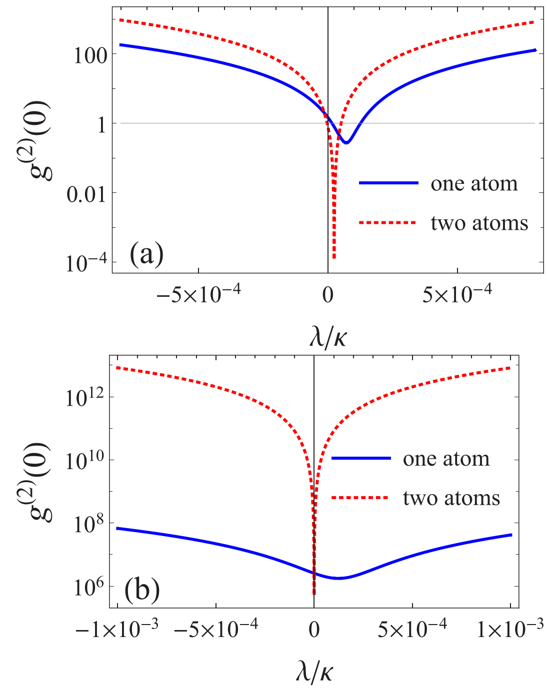

FIG. 10. Plots of the second-order correlation function $g^{(2)}(0)$ against the normalized strength of squeezed light λ/κ for the two systems ($\Delta_a = 0$ and $\Delta_c = -0.5\kappa$) for parameters $\varepsilon/\kappa = 0.01$ and $\gamma = \kappa/2$ in (a) the weak-coupling case ($g = 0.5\kappa$) and (b) the strong-coupling case ($g = 10\kappa$).

third is represented by the direct transition generated by the squeezed light $|gg, 0\rangle \rightarrow |gg, 2\rangle$, as shown by the schematic representation of Fig. 7. This last pathway transition enhances constructive quantum interference leading to antiblockade. An interesting observation is that the two-atom system is able to produce stronger antibunching than the single-atom case. Hence, the photon-blockade phenomenon is improved. This improvement is due to the enhanced destructive interference effect which results from the additional coupling provided by the two atoms. For strong coupling [Fig. 8(b)], light exhibits a very high bunching, even much higher than the single-atom cavity.

Now we consider resonance between the cavity and the driving field ($\Delta_c = 0$) [Fig. 9(a)]. The PB is clearly observed for weak coupling. Again, we notice here that the antibunching effect is stronger for the two-atom system. The increase of the light-atom coupling suppresses the antibunching effect with higher values of $g^{(2)}(0)$ in favor of the two-atom system [Fig. 9(b)].

The equal-time second-order correlation function when the coherent driving field is resonant with the atomic system ($\Delta_a = 0$) is illustrated by Fig. 10. For weak coupling [Fig. 10(a)] the value of $g^{(2)}(0)$ is of the order of 10^{-4} for the two-atom system, for very weak second-order nonlinearities. For the same system parameters, $g^{(2)}(0)$ of the single-atom system is close to 10^{-1}. Here also the collective coupling enhances the destructive interference, yielding the improvement of the PB effect. However, in the strong-coupling regime, we observe only a highly bunched state resulting from a constructive interference mechanism [Fig. 10(b)].

Optimal PB conditions, derived from Eq. (38) by setting $A_{gg,2} = 0$, can be written as

$$\lambda_{1,2} = \pm\frac{4\gamma\varepsilon^2}{\gamma(\gamma+2\kappa)+12g^2} \times \frac{\sqrt{(\gamma\kappa+16g^2)[4g^2-\gamma(\gamma+\kappa)]}}{\sqrt{(\gamma\kappa+8g^2)[\gamma(\gamma+\kappa)+4g^2]}},$$

$$\Delta_{c,1,2} = \mp\frac{\sqrt{(\gamma\kappa+8g^2)\{16g^4-[\gamma(\gamma+\kappa)]^2\}}}{2\gamma\sqrt{\gamma\kappa+16g^2}}$$

and can be approximated for weak coupling to $\lambda_{1,2} \simeq \pm 4i\varepsilon^2/(\gamma+2\kappa)$, which is the same relation as for the single two-level system. For strong coupling, it can take the form $\lambda_{1,2} \simeq \pm\sqrt{2}\gamma\varepsilon^2/3g^2$. Due to the additional coupling generated by the second two-level atom, this last condition varies in $1/g^2$. This explains the rapid attenuation of the curve in Fig. 11(a) (dotted line). The detunings $\Delta_{c,1,2}$ vary now in g^2, whereas it showed a linear evolution for the single atom [Fig. 11(b)].

In conclusion, to achieve optimal PB in the two two-level systems we need smaller second-order nonlinearities than the single-atom cavity (this is clearly observed in Fig. 10 as well as in Fig. 9 when $\Delta_c = 0$). This seems an important feature given that it may offer a supplementary solution essentially for some kinds of materials unable to produce strong squeezing. In contrast, these weak nonlinearities should be compensated by strong detunings Δ_c. In other words, for the two-atom system, the cavity should be excited far away from the resonance.

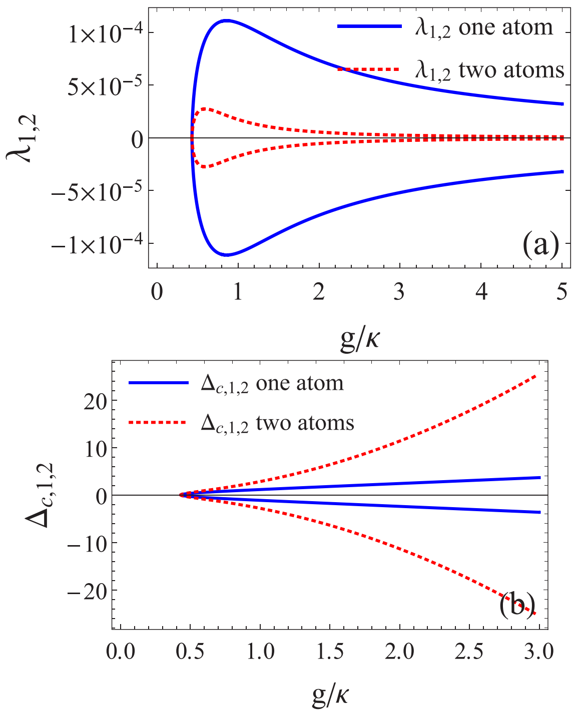

FIG. 11. Optimal PB conditions for (a) squeezed light amplitude $\lambda_{1,2}$ and (b) detunings $\Delta_{c,1,2}$ plotted as a function of the coupling strength g/κ for the two systems, with $\gamma = \kappa/2$ and $\varepsilon/\kappa = 0.01$.

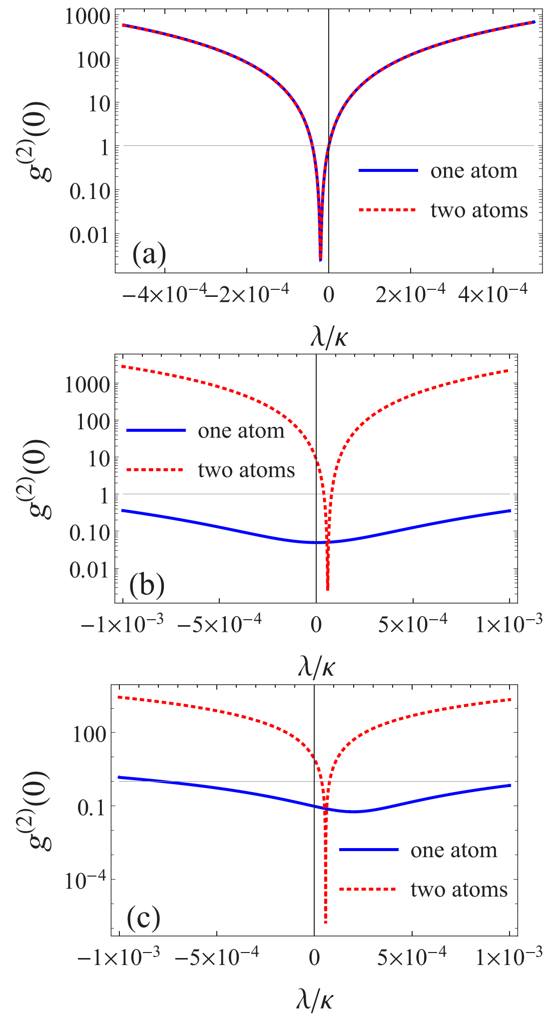

FIG. 12. Second-order correlation function $g^{(2)}(0)$ plotted versus normalized amplitude of squeezed light λ/κ for the two systems $(\Delta_a = \Delta_c = \Delta = -10\kappa)$ for the parameters $\varepsilon/\kappa = 0.01$ and $\gamma = \kappa/2$ in (a) the weak-coupling regime $(g = 0.5\kappa)$, (b) the strong-coupling regime $(g = 10\kappa)$, and (c) the strong-coupling regime $(g = 10.3\kappa)$.

We assume now that $\Delta_a = \Delta_c = \Delta$. In Fig. 12(a), which represents $g^{(2)}(0)$ as a function of the normalized amplitude of squeezed light λ/κ in the weak-coupling regime, we clearly observe that the single- and two-atom systems behave similarly. The identical curves indicate the same amount of antibunching, which corresponds to a negative second-order nonlinear susceptibility. For increasing coupling g and contrary to the previous situations of strong coupling, we can achieve a high antibunching [Fig. 12(b)]. Interestingly, this phenomenon is enhanced for the two-atom system once again.

To better see the improvement of PB outlined above due to the additional coupling resulting from the $|+, 1\rangle \leftrightarrow |ee, 0\rangle$ transition in the two-atom system, we consider the equal detuning case of Fig. 12 as an example. The rate of the $|+, 1\rangle \leftrightarrow |ee, 0\rangle$ transition is equal to $\sqrt{2}g$. For strong coupling ($g = 10\kappa$), this rate becomes important and the transition effect begins to be visible in Fig. 12(b). The further increase of the coupling strength $g = 10.3\kappa$ induces a higher antibunching. At the same moment, we notice no change of the optimal effect for the single-atom cavity [Fig. 12(c)].

IV. CONCLUSION

We have studied the PB effect in a cavity containing a two-level system and then two two-level atomic systems interacting with squeezed light through second-order nonlinearity. In the single-atom case, we found that at total resonance squeezed photons decrease the antibunching. However, for an off-resonant interaction, the effect can be strongly enhanced in the weak-coupling and strong-coupling regimes. The highest magnitude of the antibunching effect is noticed for equal detunings and for strong coupling at relatively-high-frequency detunings. In the two-atom cavity system, the PB is greatly improved compared to the single-atom case. This improvement results from the additional coupling appearing in the system due to the two atoms coupled to light.

APPENDIX: OFF-RESONANT INTERACTIONS FOR THE SINGLE-ATOM CAVITY

Here we extend the study of Sec. II to off-resonant interactions ($\Delta_a \neq \Delta_c$). We consider the weak-coupling regime at a fixed coupling strength $g = 0.45\kappa$. When there is no squeezed source interacting with the cavity [Fig. 13(a)], the density plot of the second-order correlation function shows two symmetrical branches of bunched light with respect to the origin (0, 0) and a branch around total resonance corresponding to strong antibunching. We notice that this nonclassical light is generated for the condition $\Delta_a\Delta_c \leqslant 0$. The dependence of $g^{(2)}(0)$ on the two-level system detuning Δ_a is better

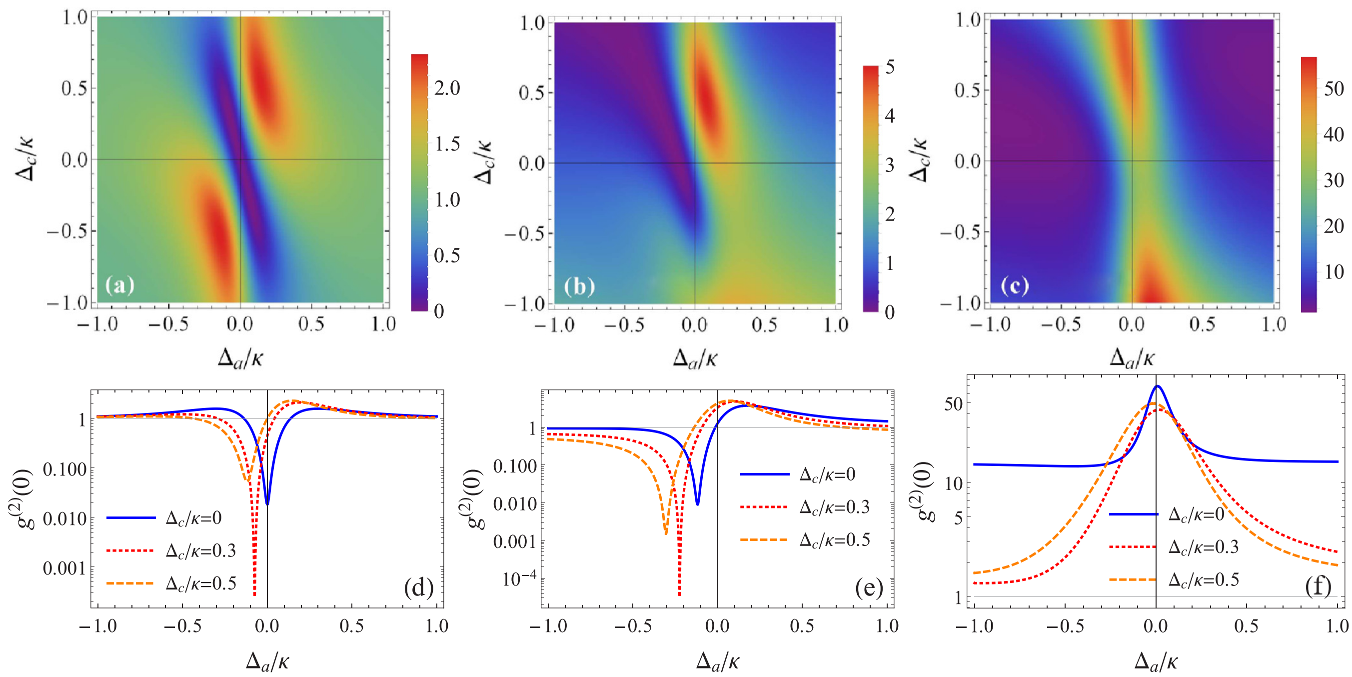

FIG. 13. (a)–(c) Density plots of the second-order correlation function $g^{(2)}(0)$ versus the normalized detunings Δ_a/κ and Δ_c/κ for $\gamma = \kappa/2$, $\varepsilon/\kappa = 0.01$, and various values of squeezed light strength λ for weak coupling given by $g/\kappa = 0.45$: (a) $\lambda = 0$, (b) $\lambda = 10^{-4}\kappa$, and (c) $\lambda = 5 \times 10^{-4}\kappa$. (d), (e), and (f) Cross sections of (a), (b), and (c), respectively, along Δ_a.

illustrated as cross sections of $g^{(2)}(0)$ for various cavity detunings Δ_c in Fig. 13(d). It can be seen that the strongest PB is achieved for slightly-off-resonant excitation, around $(\Delta_a, \Delta_c) = (-0.1\kappa, 0.3\kappa)$. When squeezed light acts on the cavity ($\lambda = 10^{-4}\kappa$), we observe two distinct branches: the first for high antibunching and the second corresponding to increasing bunching compared to the previous case [$g^{(2)}(0) = 5$]. The PB effect may reach a magnitude lower than 10^{-4} for $(\Delta_a, \Delta_c) = (-0.22\kappa, 0.3\kappa)$ [Fig. 13(e)]. Any further increase of squeezing pumping no longer improves the nonclassical effect. It simply generates highly bunched light at any given detunings [Figs. 13(c) and 13(f)].

[1] E. Knill, R. Laflamme, and G. J. Milburn, Nature (London) **409**, 46 (2001).
[2] P. Kok, W. J. Munro, K. Nemoto, T. C. Ralph, J. P. Dowling, and G. J. Milburn, Rev. Mod. Phys. **79**, 135 (2007).
[3] V. Scarani, H. Bechmann-Pasquinucci, N. J. Cerf, M. Dušek, N. Lütkenhaus, and M. Peev, Rev. Mod. Phys. **81**, 1301 (2009).
[4] V. Giovannetti, S. Lloyd, and L. Maccone, Nat. Photon. **5**, 222 (2011).
[5] A. Li, T. Chen, Y. H. Zhou, and X. B. Wang, Opt. Lett. **41**, 1921 (2016).
[6] A. Imamoglu, H. Schmidt, G. Woods, and M. Deutsch, Phys. Rev. Lett. **79**, 1467 (1997).
[7] K. M. Birnbaum, A. Boca, R. Miller, A. D. Boozer, T. E. Northup, and H. J. Kimble, Nature (London) **436**, 87 (2005).
[8] Y. X. Liu, X. W. Xu, A. Miranowicz, and F. Nori, Phys. Rev. A **89**, 043818 (2014).
[9] D. Englund, A. Majumdar, A. Faraon, M. Toishi, N. Stoltz, P. Petroff, and J. Vučković, Phys. Rev. Lett. **104**, 073904 (2010).
[10] G. W. Lin, Y. H. Qi, X. M. Lin, Y. P. Niu, and S. Q. Gong, Phys. Rev. A **92**, 043842 (2015).
[11] A. Faraon, I. Fushman, D. Englund, N. Stoltz, P. Petroff, and J. Vučković, Nat. Phys. **4**, 859 (2008).
[12] M. Koch, C. Sames, M. Balbach, H. Chibani, A. Kubanek, K. Murr, T. Wilk, and G. Rempe, Phys. Rev. Lett. **107**, 023601 (2011).
[13] Y. Yan, J. P. Zhu, and G. X. Li, Opt. Express **24**, 13590 (2016).
[14] A. J. Hoffman, S. J. Srinivasan, S. Schmidt, L. Spietz, J. Aumentado, H. E. Türeci, and A. A. Houck, Phys. Rev. Lett. **107**, 053602 (2011).
[15] A. Miranowicz, M. Paprzycka, Y. X. Liu, J. Bajer, and F. Nori, Phys. Rev. A **87**, 023809 (2013).
[16] O. Kyriienko, I. A. Shelykh, and T. C. H. Liew, Phys. Rev. A **90**, 033807 (2014).
[17] H. Wang, X. Gu, Y. X. Liu, A. Miranowicz, and F. Nori, Phys. Rev. A **92**, 033806 (2015).
[18] H. X. Zheng, D. J. Gauthier, and H. U. Baranger, Phys. Rev. Lett. **107**, 223601 (2011).
[19] D.-Y. Wang, C.-H. Bai, X. Han, S. Liu, S. Zhang, and H.-F. Wang, Opt. Lett. **45**, 2604 (2020).
[20] A. Majumdar and D. Gerace, Phys. Rev. B **87**, 235319 (2013).
[21] H. Z. Shen, Y. H. Zhou, H. D. Liu, G. C. Wang, and X. X. Yi, Opt. Express **23**, 32835 (2015).
[22] H. Flayac and V. Savona, Phys. Rev. A **88**, 033836 (2013).
[23] S. Ferretti, V. Savona, and D. Gerace, New J. Phys. **15**, 025012 (2013).

[24] O. Kyriienko and T. C. H. Liew, Phys. Rev. A **90**, 063805 (2014).
[25] T. C. H. Liew and V. Savona, Phys. Rev. Lett. **104**, 183601 (2010).
[26] M. Bamba, A. Imamoglu, I. Carusotto, and C. Ciuti, Phys. Rev. A **83**, 021802 (2011).
[27] A. Majumdar, M. Bajcsy, A. Rundquist, and J. Vučković, Phys. Rev. Lett. **108**, 183601 (2012).
[28] D. Gerace and V. Savona, Phys. Rev. A **89**, 031803(R) (2014).
[29] H. Flayac and V. Savona, Phys. Rev. A **96**, 053810 (2017).
[30] E. Z. Casalengua, J. C. L. Carreño, F. P. Laussy, and E. del Valle, Laser Photon. Rev. **14**, 1900279 (2020).
[31] D. F. Walls, Nature (London) **306**, 141 (1983).
[32] V. Dodonov, J. Opt. B **4**, R1 (2002).
[33] A. H. Safavi-Naeini, T. P. Mayer Alegre, J. Chan, M. Eichenfield, M. Winger, Q. Lin, J. T. Hill, D. E. Chang, and O. Painter, Nature (London) **472**, 69 (2011).
[34] I. Pikovski, M. R. Vanner, M. Aspelmeyer, M. S. Kim, and C. Brukner, Nat. Phys. **8**, 393 (2012).
[35] J. Paramanandam and M. A. Parker, Phys. Rev. Lett. **94**, 233602 (2005).
[36] Y. Zhao, N. Aritomi, E. Capocasa, M. Leonardi, M. Eisenmann, Y. Guo, E. Polini, A. Tomura, K. Arai, Y. Aso, Y.-C. Huang, R.-K. Lee, H. Lück, O. Miyakawa, P. Prat, A. Shoda, M. Tacca, R. Takahashi, H. Vahlbruch, M. Vardaro *et al.*, Phys. Rev. Lett. **124**, 171101 (2020).
[37] L. McCuller, C. Whittle, D. Ganapathy, K. Komori, M. Tse, A. Fernandez-Galiana, L. Barsotti, P. Fritschel, M. MacInnis, F. Matichard, K. Mason, N. Mavalvala, R. Mittleman, H. Yu, M. E. Zucker, and M. Evans, Phys. Rev. Lett. **124**, 171102 (2020).
[38] K. Fukui, A. Tomita, A. Okamoto, and K. Fujii, Phys. Rev. X **8**, 021054 (2018).
[39] T. Douce, D. Markham, E. Kashefi, E. Diamanti, T. Coudreau, P. Milman, P. van Loock, and G. Ferrini, Phys. Rev. Lett. **118**, 070503 (2017).
[40] J. M. Arrazola, V. Bergholm, K. Brádler, T. R. Bromley, M. J. Collins, I. Dhand, A. Fumagalli, T. Gerrits, A. Goussev, L. G. Helt, J. Hundal, T. Isacsson, R. B. Israel, J. Izaac, S. Jahangiri, R. Janik, N. Killoran, S. P. Kumar, J. Lavoie, A. E. Lita *et al.*, Nature (London) **591**, 54 (2021).
[41] E. A. Sete and H. Eleuch, Phys. Rev. A **89**, 013841 (2014).
[42] J. Aasi, Nat. Photon. **7**, 613 (2013).
[43] H. Grote, K. Danzmann, K. L. Dooley, R. Schnabel, J. Slutsky, and H. Vahlbruch, Phys. Rev. Lett. **110**, 181101 (2013).
[44] K. Vahala, *Optical Microcavities* (World Scientific, Singapore, 2004).
[45] B. Deveaud, *The Physics of Semiconductor Microcavities* (Wiley, New York, 2007).
[46] J. P. Karr, A. Baas, R. Houdré, and E. Giacobino, Phys. Rev. A **69**, 031802(R) (2004).
[47] H. Jabri and H. Eleuch, Phys. Rev. A **101**, 053819 (2020).
[48] H. Jabri and H. Eleuch, Phys. Rev. A **102**, 063713 (2020).
[49] H. Jabri and H. Eleuch, Sci. Rep. **12**, 3658 (2022).
[50] M. T. Johnsson and S. A. Haine, Phys. Rev. Lett. **99**, 010401 (2007).
[51] H. Jabri, H. Eleuch, and T. Djerad, Laser Phys. Lett. **2**, 253 (2005).
[52] C. H. H. Schulte, J. Hansom, A. E. Jones, C. Matthiesen, C. Le Gall, and M. Atatüre, Nature (London) **525**, 222 (2015).
[53] H. A. R. El-Ella, Phys. Rev. A **103**, 023701 (2021).
[54] P. Scholl, H. J. Williams, G. Bornet, F. Wallner, D. Barredo, L. Henriet, A. Signoles, C. Hainaut, T. Franz, S. Geier, A. Tebben, A. Salzinger, G. Zürn, T. Lahaye, M. Weidemüller, and A. Browaeys, PRX Quantum **3**, 020303 (2022).
[55] L. C. G. Govia, A. Lingenfelter, and A. A. Clerk, Phys. Rev. Research **4**, 023010 (2022).
[56] H. J. Carmichael, R. J. Brecha, and P. R. Rice, Opt. Commun. **82**, 73 (1991).
[57] J. Tang, W. Geng, and X. Xu, Sci. Rep. **5**, 9252 (2015).